OPTICAL PROPERTIES OF SMALL MINERAL DUST PARTICLES AT VISIBLE/NEAR-IR WAVELENGTHS: NUMERICAL CALCULATION AND LABORATORY MEASUREMENT

Robert A. West[1], Martin G. Tomasko[2], and Lyn R. Doose[2]

[1]Jet Propulsion Laboratory, California Institute of Technology, Pasadena, CA
[2]Lunar and Planetary Laboratory, University of Arizona, Tuscon, Arizona

1. INTRODUCTION

Remote sensing studies of the land, ocean, and atmosphere are affected by aerosol loading in the atmosphere. An accurate accounting of the radiative effects of aerosols requires an accurate model for aerosol optical properties. The traditional approach using Mie theory for spheres is inappropriate when the aerosol is a mineral dust (a frequent situation downwind of desert areas). To better understand the optical properties of mineral dust we computed optical properties for a variety of particle shapes and sizes up to equivalent-volume size parameter $X = 2\pi r/\lambda = 8$, and we are performing laboratory measurements on a variety of mineral powders in the same size regime and somewhat larger. The laboratory results are not yet available, and so this paper presents results only for the numerical calculations. The optical parameters most important to remote sensing measurements are the aerosol extinction, scattering, and absorption optical depths, and the particle scattering phase function (the P_{11} term of the phase matrix), and the linear polarization (defined as $-100 \times P_{11}(\theta)/P_{12}(\theta)$, where P_{11} and P_{12} are scattering phase matrix elements, and θ is the scattering angle.

2. COMPUTATIONAL METHOD

The computations use a discrete-dipole approach (Goodman et al., 1991) and give information on optical cross sections and all phase matrix elements. The particles can have arbitrary shape and composition. The computing time scales as a power of the particle volume. The largest particles in this study have volumes equal to a sphere with size parameter X = 8. By comparison with Mie theory, the calculations are accurate to a few percent in optical cross section and phase function, and to about 10% or better for polarization.

Computing time is long for the largest particles, and so the study was limited to a few particle types and a single refractive index, m = (1.5323,0.008), typical of desert dust at red wavelengths (d'Almeida et al., 1991). Dust particles come in an infinite variety of shapes, but almost always are multi-faceted angular fragments (as opposed to smooth spheroids). It is difficult to know the optimum choice of particle shape when conclusions must be based on a few cases. For simplicity we started with a rectangular prism with edges in the ratio 2:3:4, a hexagonal prism with edges in the ratio 19:9 (the 9 edge is parallel to the six-fold symmetry axis and the 19 edge is perpendicular to it), and a tetrahedron having four equilateral triangle faces. These particles provided for a range in aspect ratio, with the greatest being that for the hexagonal prism (the maximum cord length across the hexagon is 38 in the same units as before). They also provided a variety of dihedral angles and number of facets.

Calculations were made for 9 orientations of the particle and averaged to approximate random orientation. Results were computed for a grid in equivalent-volume X parameter, ranging from 0.1 to 8 (7 for the tetrahedron) in steps of a factor of 1.1. Optical properties for log-normal size distributions, truncated on the large end at X = 7, were derived by interpolating and summing among the table entries over the grid on X. The resulting phase functions were compared with the identical size distribution for spheres, using Mie theory.

3. RESULTS

Extinction cross sections for the three shapes are almost identical, rising as a steep function of X up to X = 4, where the extinction efficiency (ratio of the extinction cross section to the geometric cross section) reaches a maximum of 4 for spheres, tetrahedra, and brick-shaped particles. At X larger than 5 the extinction efficiency for spheres, tetrahedral and bricks decreases with X, but less rapidly for nonspherical particles. The hexagonal prism particles actually show a slight increase in extinction efficiency up to X = 8.

Particle scattering phase functions become more

Robert A. West, MS 169-237 Jet Propulsion Lab, 4800 Oak Grove Dr., Pasadena, CA91109

forward scattering as X increases, due chiefly to forward scattering diffraction, The diffraction pattern depends on the projected area cross sections, and so it is expected that particles with equal projected area should have similar forward scattering lobes. This is borne out in the calculations for nonspherical particles in the scattering angle range 0°-700, although significant differences are apparent for the different particle shapes.

Scattering phase functions for two size distributions are shown in Figs. 1 and 2. In the figures Xeff is the effective (scattering cross-section weighted X value) for ,X computed for equal projected area particles. The effective variance of the distribution is show as Veff. The distributions are log-normal with a cutoff at X = 7. The brick and tetrahedral particles have projected area effective radii which are 1.094 and 1.066 times the equal-area sphere, whereas the hexagonal prism has an effective radius 1.2 times that for an equal projected area sphere. The brick and tetrahedron phase functions are very similar to that for the sphere, but even at relatively small Xeff (Xeff = 1.74 in Fig. 1) the tetrahedron shows 20-30% differences at low and intermediate scattering angles.

Spherical particles develop glory backscattering lobes at the larger X values (Xeff = 4.3 in Fig. 2), while the nonspherical particles examined here have only small enhancement in the scattering angle range 165° – 180°. Faceted particles have phase functions which are factors of 3-5 higher than for spheres at scattering angles greater than 150°. Differences between the three nonspherical particles are as large as a factor of 2 at scattering angles between 60° – 180°. The hexagonal prism with the highest aspect ratio shows the largest difference, Remote sensing measurements of the phase function behavior in the scattering angle range 110”-150° should be the most sensitive to sphere us nonsphere.

The linear polarizing properties of the particles are extremely sensitive to shape. Linear polarization (see parts b of Figs. 1 and 2) remains positive at intermediate angles up to larger X values than for non-spheres. A weak negative branch can develop at large scattering angles when Xeff is larger than about 3.5, depending on the shape. Spherical particles of the same size have strong negative polarization at scattering angles between 150° and 165°

Acknowledgments: We thank B. Draine, P. Flatau, and J. Goodman for providing their discrete-dipole code. ‘This work was performed in part by the Jet Propulsion Laboratory, California Institute of Technology, under contract with the National Aeronautics and Space Administration.

REFERENCES

d’Almeida, G. A., P. Koepke, and E. P. Shettle, 1991 Atmospheric Aerosols Global Climatology and Radiative Characteristics. A. Deepak Publishing, Hampton, Virginia.

Goodman, J. J., B. ‘1’. Draine, and P. J. Flatau, 1991 Application of fast-Fourier-transform techniques to the discrete-dipole approximation. *Optics Let., 16,* 1198-1200.

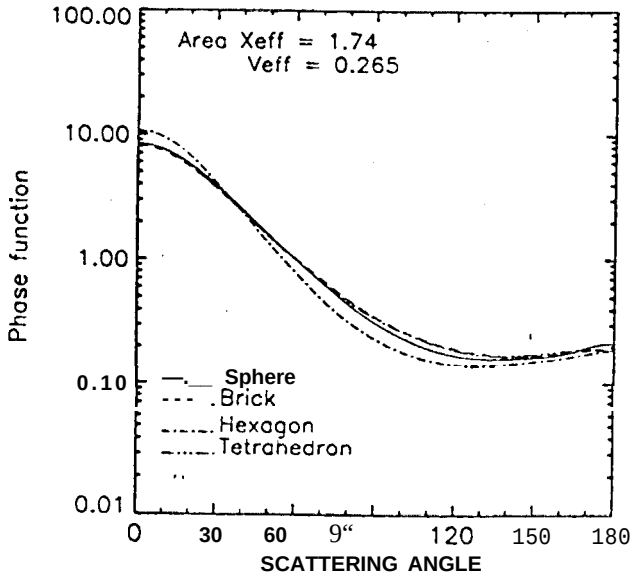

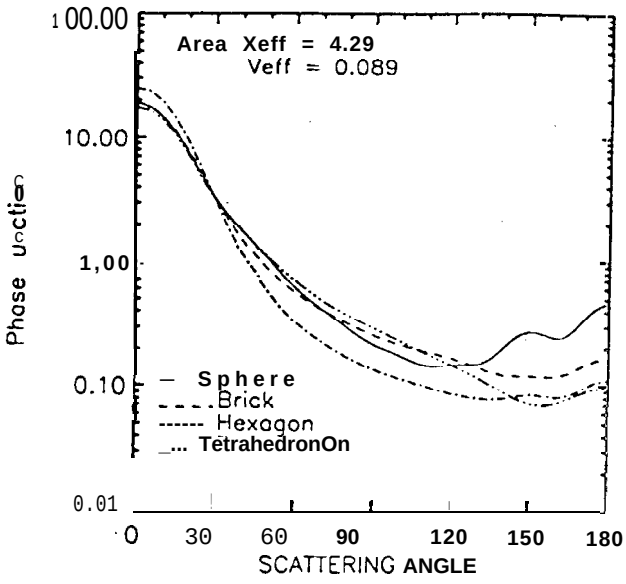

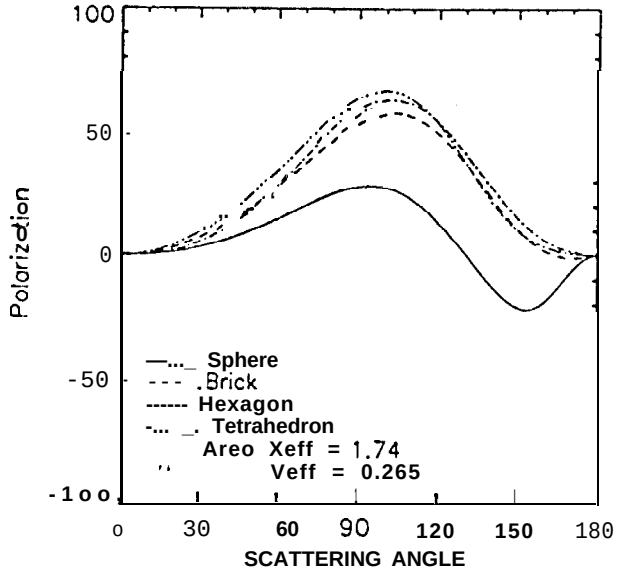

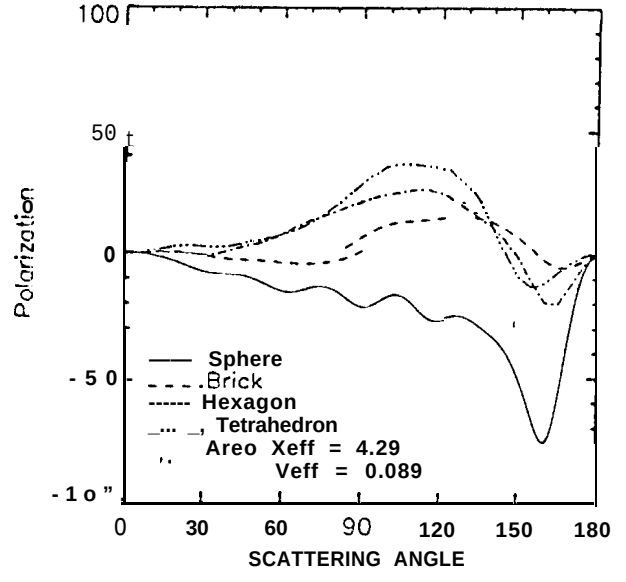

Figure 1: Scat, tering phase function (top panel) and linear polarization for four particle shapes. The size distribution is a log-normal with equal projected area effective X and variance parameters as indicated.

Figure 2: Scattering phase function and linear polarization for four particle shapes, with a larger effective radius and smaller variance than in fig. 1. All particles have refractive index m = (1.5323, 0.008)